Gas6/Axl is the sensor of Arginine-Auxotrophic Response in Targeted Chemotherapy with Arginine-Depleting Agents

Wen-Bin Tsai[1], **Yan Long**[1], **Jeong-Ran Park**[2], **Jeffrey T. Chang**[3], **Hui Liu**[1], **Jaime Rodriguez-Canales**[1], **Niramol Savaraj**[4], **Lynn G. Feun**[5], **Michael A. Davies**[6], **Ignacio I Wistuba**[1], and **Macus Tien Kuo**[1]

[1]Department of Translational Molecular Pathology, The University of Texas MD Anderson Cancer Center, Houston, Texas 77030

[2]Department of Thoracic and Cardiovascular Surgery, Kangwon National University, Gangwon, Korea 200-701

[3]Department of Integrative Biology and Pharmacology, University of Texas Health Science Center at Houston, Houston, Texas 77030

[4]Sylvester Comprehensive Cancer Center, University of Miami, Miami, FL 33135

[5]Sylvester Comprehensive Cancer Center, University of Miami, VA Medical Center, Miami, Fl. 33125

[6]Department of Melanoma Medical Oncology, The University of Texas MD Anderson Cancer Center, Houston, Texas 77030

Abstract

Many human malignancies lack *de novo* biosynthesis of arginine (Arg) because the key enzyme argininosuccinate synthetase 1 (ASS1) is silenced. These tumors acquire ectopic Arg for survival, and depleting this source by Arg-depleting recombinant enzyme ADI-PEG20 results in cell death. Mechanisms underlying Arg auxotrophy in these tumors and how they respond to Arg-auxotrophic stress are poorly understood. Here, we report that an immediate early event of Arg-auxotrophic response involves ROS-mediated secretion of Gas6 which interacts with its receptor Axl and activates the downstream Ras/PI3K/Akt growth signal leading to accumulation of c-Myc by protein stabilization. Arg-auxotrophic challenge also transcriptionally upregulates c-Myc expression which feedbacks to enhance Axl expression. c-Myc is a positive regulator of ASS1, but elevated ASS1 feedbacks to suppress c-Myc and Axl. Our results revealed multiple inter-regulatory pathways in Arg-auxotrophic response consisting of Axl, c-Myc, ASS1 that regulate Arg homeostasis and ADI-PEG20 sensitivity. These pathways provide potential targets for improving the efficacy of treating Arg-auxotrophic tumors using Arg deprivation strategies.

Corresponding Author: Dr. Macus Tien Kuo, Department of Translational Molecular Pathology, The University of Texas MD Anderson Cancer Center, 2130 W. Holcombe Blvd, Life Science Plaza LSP9.4206, Houston, Texas 77030. Phone: 713-835-6038; Fax: 713-834-6085; tkuo@mdanderson.org.

Keywords

Gas6; Axl; Arginine; c-Myc; ROS; ADI-PEG20

INTRODUCTION

L-arginine (Arg) is a semi-essential amino acid. Malignant cells require sufficient amounts of Arg for protein biosynthesis to sustain their highly proliferative activity. Arg can be *de novo* synthesized from citrulline and aspartate by argininosuccinate synthetase 1 (ASS1). ASS1 deficiency causes citrullinemia, a rare autosomal recessive disease [3]. Alternatively, Arg can be obtained from the extracellular milieu through cationic amino acid transporters. It has been reported that subpopulations of various human malignancies in many different lineages do not produce sustainable amounts of Arg and require extracellular Arg for survival, because these tumors express very low levels of ASS1[12, 34]. The Arg-degrading recombinant enzymes, pegylated arginine deiminase (ADI-PEG20, hereafter ADI) which digests Arg into citrulline and ammonia, and human arginase 1 which digests Arg into ornithine and urea, induce Arg-auxotrophic stress, leading to cell death (see references in reviews [12, 34]). These recombinant proteins have been in various stages of clinical development for targeting Arg-auxotrophic tumors [43]. An important mechanism of Arg-auxotrophic response is induction of ASS1 expression, resulting in resistance to Arg-deprivation treatment.

We previously demonstrated that induction of ASS1 expression by Arg deprivation involves de-repression of HIF-1α by downregulation but upregulation of c-Myc, which replaces HIF-1α to upregulate ASS1 expression [58]. We further demonstrated that upregulation of c-Myc follows the signal transduction mechanism involving Ras→PI3K/Akt/ERK→GSK3β, where ERK phosphorylates c-Myc, resulting in c-Myc accumulation by suppressing proteasomal degradation [59]. However, how Arg-auxotrophic stress is sensed in activating the Ras signal is not known.

We report here that ROS-related immediate-early activation of Gas6/Axl followed by a c-Myc-mediated transcriptional upregulation of Axl is involved in Arg-auxotrophic response leading to enhanced expression of ASS1. Elevated ASS1 expression provides feedback and suppresses c-Myc and Axl expression, constituting a self-regulatory mechanism of Arg-auxotrophic management that has implications for targeted therapy of Arg-auxotrophic tumors.

RESULTS

Activation of Axl in response to ADI in melanoma cells

To investigate whether activation of receptor tyrosine kinases (RTK) is involved in Arg-auxotrophic response that activates Ras signaling[59], we used lysates of A2058 cells treated with or without ADI for 15 min to probe an array of 42 anti-phosphotyrosine receptor antibodies in duplicate and observed that Axl was the predominant RTK activated (Fig. 1A). We confirmed this using Western blotting which demonstrated a dose-dependent activation

of Axl by ADI (Fig.1B). Activated Axl in A2058 cells can be seen as early as 5 min after ADI treatment but disappears after 30 min of exposure (Fig. 1C). This transient induction of Axl was also seen in A2058 cells grown in Arg-free medium (Fig. 1D). Activation of Axl by ADI was also seen in another melanoma cell line SK-Mel-2 (not shown) and in breast cancer cell line MDA-MB-231 but the kinetics of induction was delayed and persistent through an 1-hr treatment (Fig. 1E). No activation of Axl and Akt was seen in A375 cells (Fig. 1F), consistent with our previous observations for the non-inducibility of this cell line by ADI-treatment [59]. These observations revealed substantial heterogeneity in response to Arg-deprivation in human cancer cell lines. Moreover, while no p-Axl was detectable in A2058 cells treated with ADI or grown in Arg(−) conditions after 30 min treatments, p-Akt levels continued to increase thereafter, suggesting that activation of Akt is a downstream event.

To demonstrate the role of Axl in Arg-auxotrophic response, we introduced the dominant-negative Myc-tag Axl mutant (Axl-DN-Myc, K558R in the kinase domain). Overexpression of Axl-DN-Myc abolished the ADI-induced Ras/Akt signal (Fig. 1G). Axl is a membrane-bound RTK with extracellularly located ligand-binding domain. A truncated form of human Axl known as soluble Axl (sAxl) containing extracellular ligand-binding domains was found in plasma of leukemia patients [8]. sAxl acts as a "sponge" to neutralize Gas6 by preventing it from binding to the native Axl receptor. Expression of sAxl suppresses Axl signaling induced by ADI (Fig. 1H). These results demonstrated that Axl plays an important role in Arg-auxotrophic response.

Gas6 secretion leads to Axl activation in response to ADI treatment

The ligand of Axl is Gas6 [8]. Because melanoma cells, including those described in this study, express undetectable amount of Gas6 by Western blotting, we used MDA-MB-231 cells which express high amount of Gas6 and is also auxotrophic for Arg [59]. Axl activation can be ligand-dependent or -independent. Because the ligand-binding domain of Axl is extracellularly located, ligand-dependent activation of Axl requires Gas6 externalization. We treated MDA-MB-231 cells with ADI for different lengths of time. We found a time-dependent reduction of cellular Gas6 (endo-Gas6) with correspondingly increased ectopic Gas6 in culture media (ex-Gas6) (Fig. 2A). For Gas6 to interact with Axl, Gas6 has to be enriched in plasma membrane. To demonstrate enhanced membrane association of Gas6 in ADI treatment, we fractionated cell lysates into cytoplasmic (C), membrane (M), and nuclear (N) fractions. Cross-contamination in these three fractions was minimal as evidenced by the distributions of α-tubulin for cytosol, Na^+/K^+ ATPase for membrane and lamin B for nucleus as markers. We found that ADI treatment resulted in Gas6 enrichment in the membrane fraction, whereas p-Akt and c-Myc enrichment in the nuclear fraction (Fig. 2B). These results demonstrated that ADI triggers Gas6 release into medium to activate Axl. The importance of Gas6 in Arg-auxotrophic response was further demonstrated using two Gas6 shRNA showing that knockdown of Gas6 abolished Axl activation (Fig. 2C), whereas overexpression of Gas6 enhanced Axl activation (Fig. 2D).

Gas6 has two important structural features for its bioactivity. The C-terminus contains "sex-hormone-binding globulin" domain which binds to the Ig domains of the receptor. The N-terminus of Gas6 is rich in glutamic acids (Gla domain)[49]. The γ-hydroxyl groups of these

glutamic acid residues are posttranslationally carboxylated in a vitamin K-dependent modification. We used the Gas6 inhibitor warfarin, which inhibits γ-glutamylcarboxyltransferase and prevents γ-carboxylation of Gas6 [21]. We found that warfarin suppressed ADI-induced Axl activation (Fig. 2E). Combination of warfarin and ADI exhibits additive cell-killing effects as determined by SRB (Fig. 2F) and apoptosis (DNA fragmentation) assays (Fig. 2G).

Many small molecules have been developed to inhibit RTKs and some have been shown against Axl, although no inhibitor has been demonstrated clearly Axl-specific [11]. SKI-606 (bosutinib) is an FDA and European Medicines Agency (EMA) approved agent for treating Ph+ CML that mainly targets Bcr-Abl and Src, and to a lesser extent, Axl [27, 56, 65]. As proof of principle, we found that SKI-606 suppressed ADI-induced Axl activation and its downstream signal (Fig. 2H). SKI-606 enhanced ADI's cell-killing capacity (Fig. 2I) by enhanced apoptosis mechanism (Fig. 2J). Taken together, these results demonstrated that Gas6/Axl are potential targets for Arg starvation therapy.

Elevated expression of Gas6/Axl in ADI-resistant cell lines

We previously established 5 independent ADI-resistant variants (ADI[R]) in A2058 background (A2058R1 – R5) that resist to ADI treatment [37] (Fig. 2K). All these ADI[R] variants exhibited elevated Gas6 and Axl along with the downstream signals, Akt, ERK and ASS1, their expression levels were not strictly correlated with Gas6 and p-Axl/Axl levels, reflecting clonal heterogeneity among these cell lines (Fig. 2L) In addition, all ADI[R] cells are sensitive to SKI-606 (Fig. 2M). Knockdown of Axl diminished these downstream signals (Fig. 2N and Fig. S3) and rendered the ADI[R] cells sensitive to ADI treatment (Figs. 2O and 2P, and S4). These results further supported the roles of Gas6/Axl in Arg auxotrophic response and in ADI resistance.

Gas6 secretion induced by ADI follows conventional protein translocation mechanism that is regulated by ADI-induced ROS

Under non-stressed conditions, γ-carboxylation of Gla domain allows Gas6 to bind to phosphatidylserine (PtdSer) at the inner-, cytoplasm-facing leaflet of the plasma membrane under the control of P4-ATPases or flippases and plasma membrane scramblases [31, 54]. In an apoptotic cell, PtdSer is displayed on the extracellular membrane surface because of disable of flippases and enhanced phospholipid scramblases [50], resulting in externalization of Gas6 [17, 36]. To investigate whether Gas6 externalization follows unconventional membrane translocation mechanism or by conventional protein translocation mechanism which requires a N-terminal signal (leader) sequence that navigates secretory protein to the cell surface through the vesicular secretion pathway via endoplasmic reticulum (ER) and Golgi apparatus. Unconventional secretory proteins lack signal peptides and their transport is not affected by inhibitors to ER/Golgi [40]. Using SignalP-20 program (http://www.cbs.dtu.dk/services/SignalP/), we found that Gas6 contains a 32-amino acid signal peptide sequence located at the N-terminus (Fig. S5). We found that treating MDA-MB-231 cells with brefeldin A (BFA) which is a potent inhibitor of protein secretion by inducing Golgi dissembles [5], and golgicide A which is a highly specific inhibitor of Golgi BFA resistance

factor 1 [47], suppressed ADI-induced Gas6 externalization (Fig. 3A). These results suggested that ADI-induced Gas6 release follows a conventional secretory pathway.

Gas6 contains at many cysteine residues (amino acids 119, 124, 141, 142, 158, 164, 168,177, 283, 570 that could be involved in bisulfide linkages for Gas6 function [48]. These bisulfide bridges could be sensitive to oxidative regulation. We hypothesized that ADI treatment generates ROS to promote Gas6 secretion. Because induction of Gas6 release by ADI occurs within minutes, we preloaded MDA-MB-231 cells and A375 cells with the ROS probe dihydrorhodamine for 30 min. We found a time-dependent increased ROS production following ADI treatment in MDA-MB-231 cells is an immediate early event (Fig. 3B, left). ADI treatment of A375 cells seems reduced ROS levels, i.e., a left-shift of the fluorescence profiles (Fig. 3B, right). These findings are consistent with the differential inducibility of Gas6/Axl by ADI between these two cell lines (Figs. 1E & 1F). Although the magnitudes of ROS induction using this assay system were minor, the results are reproducible (3 experiments) and also are consistent with the recent published results using longer treatment time of ADI (see below). We next investigated whether ADI-mediated oxidative status affects Gas6 secretion. Treating MDA-MB-231 cells with antioxidant N-acetyl-L-cysteine (NAC) reduced ADI-induced Gas6 release as well as endogenous Gas6 level, whereas treating with pro-oxidants N-ethylmaleimide (NEM) or H_2O_2 promote Gas6 release and activation of the Axl signal (Fig. 3C). These results suggested that ADI-induced Gas6 secretion is mediated by a ROS-related mechanism. While the precise mechanism how NAC alone reduces Gas6 expression is unknown, but may be due to the unstable nature of Gas6 under reducing conditions (disruption of the disulfide bridge) because Gas6 is a redox-sensitive protein [32].

Shp2 is an integral part of the Gas6/Axl activation signal

To elucidate how Gas6/Axl activation transmits into its downstream Ras/Akt signals, we performed immunoprecipitation (IP) of lysates from ADI-treated or -untreated cells with anti-Axl antibody followed by Western blotting. While Gas6 was co-precipitated with Axl in the untreated cells, ADI treatment enriched Gas6 association with Axl and the Src homology-2 domain-containing protein tyrosine phosphatase 2 (Shp2) which has been demonstrated to transmit activated RTK signal to Ras/PI3K/Akt [39] (Fig. 4A). To strengthen these findings, we carried out similar experiment in a time-course manner. We found that kinetics of Axl, Gas6 and Shp2 associations mirror the kinetics of p-Axl induction in MDA-MB-231 cells (Figs. 4B and 1E). Likewise, Shp2 immunoprecipitates probed by Axl or phorphorylated tyrosine (p-Tyr) antibodies in lysates prepared from a time-course treatments of A2058 cells with ADI also follows the kinetics of p-Axl activation in this cell line (Figs. 4C and 1C). Similar results were obtained using anti-p-Tyr in immunoprecipitation followed by Western blotting with anti-Shp2 and anti-Axl antibodies (Fig. 4C).

To demonstrate the role of Shp2 in ADI-induced Gas6/Axl signal, we used a Shp2-DN which contains a catalytically inactive mutation (C459S). Expression of C459S-mutant abolished ADI-mediated Ras/Akt activation (Fig. 4D). Similar results were observed using an shRNA approach (Fig. 4E). Overexpression of wild-type Shp2 induces Akt activation

regardless of ADI treatment (Fig. 4F). These results demonstrated involvement of Shp2 in activation of Gas6/Axl/Ras/Akt signaling in response to ADI.

c-Myc is involved in transcriptional regulation of Axl expression by ADI

Activation of Gas6/Axl to Arg-auxotrophic challenge occurs within minutes. However, we found that longer challenge increased the expression of Axl and several downstream effectors as determined by Western blotting (Fig. 5). Induction of Axl by ADI was also observed at the mRNA levels measured by quantitative real-time PCR (Fig. 5B), suggesting that transcriptional regulation is involved.

In examining the proximal *Axl* promoter sequence, we found three putative E-box sequences located within −1495 nt from the transcriptional start site, designated E-box 1, E-box 2 and E-box 3 from the 5' side. We constructed reporter recombinants containing their respective wild-type E box sequences and mutations at each of these boxes (Fig. 5C, underscored). We transfected these recombinant DNA into A2058 cells and treated with ADI or grown them in Arg-free medium. Fig. 5D shows that these treatments enhanced expression of the wild-type reporter, but not in all the three mutants (mE1 etc), demonstrating that these E-boxes are involved in transcriptional regulation of *Axl* by ADI. Since c-Myc is a transcriptional regulator that interacts with E-box sequences, we hypothesized that c-Myc is involved in the transcriptional regulation of Axl by ADI. Chromatin immunoprecipitation (ChIP) demonstrated enhanced c-Myc binding to each of these E-boxes (Fig. 5E). Moreover, depleting c-Myc using shRNA approach suppressed Axl induction by ADI in the reporter assay (Fig. 5F) and in cultured cells (Fig. 5G). These results demonstrated that c-Myc transcriptionally upregulates Axl expression under Arg-auxotrophic stress conditions.

The inter-regulatory network of c-Myc, Axl, and ASS1 in Arg auxotrophic response

We previously demonstrated that ADI treatment enhanced c-Myc accumulation by inhibiting the proteasomal degradation mechanism [59]. Using quantitative real-time PCR, we observed that c-Myc mRNA was induced by ADI within 24 hr after ADI treatment (Fig. 6A). We hypothesized that enhanced c-Myc mRNA levels by ADI is auto-regulated through the E-box located −2274 nt at the 5' side of *c-Myc*. We constructed reporter plasmids containing wild-type E-box and the mutant form (Fig. 6B). While expression of the reporter in wild-type construct was induced in A2058 cells under Arg-deprivation conditions, mutation at this site reduced the expression levels (Fig. 6C). Knockdown of c-Myc in the transfected cells also diminished levels of reporter induction under these treatments (Fig. 6D). Furthermore, a ChIP assay demonstrated enhanced binding of c-Myc to the E-boxes located at the *c-Myc* promoter and *ASS1* promoter (positive control) (Fig. 6E). These results demonstrated that ADI-induced c-Myc expression is transcriptionally auto-regulated itself.

ADI-induced c-Myc expression moves forward to induce ASS1 expression [58, 59]. Using a transfection approach, we observed that overexpression of ASS1 can feed-back to limit c-Myc and Axl expression in Western blotting assay (Fig. 6F). Suppression of c-Myc and Axl expression by the elevated ASS1 is transcriptionally regulated as demonstrated by ChIP assay which shows reduced bindings of c-Myc to the E-boxes located in their respective promoters (Fig. 6G), and by reporter assay using Myc-2791-Luc and Axl-1495-Luc

reporters, respectively (Fig. 6H). Taken together, these results support feedback regulation of *c-Myc* and *Axl* by ASS1.

Reduced Gas6/Axl expression is associated with Arg-auxotrophy in melanoma cells

The above results suggest that deficiency of Gas6/Axl signal is an important mechanism of Arg-auxotrophicity. To substantiate this finding, we performed Western analyses of Gas6, Axl, and ASS1 in a panel of 15 melanoma cell lines (Fig. 7A, lanes 1-15). We found that, except SB2 line (lane 15) which expresses detectable Axl, all other cell lines express much reduced Axl. Expression of Axl in A2058, A375, and SK-Mel-2 could only be seen on autoradiograms upon long-term exposure, whereas Gas6 and ASS1 expression was virtually undetectable in all melanoma cell lines even upon prolong exposure using MDA-MB-231 breast and SKOV3 ovarian cancer cell lines as references (Fig. 7A). Ectopic expression of recombinant Gas6 in 6 randomly selected melanoma cell lines conferred Axl activation by ADI in all these cell lines (Fig. 7B), demonstrating that Gas6 controls Arg-auxotrophic response.

Correlations of Gas6, Axl, and ASS1 expression in melanoma tissues

We immunostained an array of 96 tissue specimens in duplicates from 48 individuals, consisting of 4 normal skin, 4 benign hyperplasia, 2 basal cell carcinoma, 2 squamous cell carcinoma, 24 primary melanoma and 12 metastatic melanoma. We found that Gas6 expression was virtually not detectable except one case with basal cell carcinoma. Axl expression was also undetectable except low levels expression in one each of benign and basal cell carcinoma, and 2 cases in primary melanoma. ASS1 expression was undetectable in all the melanoma. Examples of Gas6, Axl and ASS1 IHC are shown in Fig. 7C. using either MDA-MB-231 or kidney tissue as positive controls and A2058 cells as negative control for these stainings. We also ruled out the contribution of melanin in IHC, because no staining was observed using H&E staining. Collectively, these results demonstrated that Gas6, Axl and ASS1 expression levels were low in human melanoma tissues, consistent with the cell line data.

We next examined the expression levels of these genes in human melanoma tissues using the data from the TCGA database. We found that the expression of Gas6, Axl and ASS1 in 103 skin cutaneous melanoma are significantly low, compared against the expression in ovarian cancers as a baseline (data not shown). Moreover, we found that expression levels between Gas6 and Axl mRNA (Fig. 7D, left) and between Gas6 and ASS1 mRNA (Fig. 7D, middle) show significantly positive correlation ($p = 0.003$, $p < 0.0001$, respectively), whereas the correlation between Axl and ASS1 mRNA had borderline significance (Fig. 7D, right, p=0.045). For comparisons, we found significantly positive correlation between Gas6 and Axl and between Gas6 and ASS1 mRNA (both p<0.0001), whereas no correlation between Axl and ASS1 mRNA (p=0.12), in ovarian cancers (not shown). These results have important implications of the Gas6/Axl/ASS1 axis in Arg auxotrophicity in malignant melanoma. The poor correlation between Axl and ASS1 expression may suggest that multiple mechanisms are involved in the regulation of these genes in other tumor types. While little is known about Axl regulation, previous studies showed that multiple mechanisms are involved in *ASS1* regulation, including DNA methylation [55], Ca^{2+}-

dependent PKCα-mediated protein phosphorylation [19], cAMP-mediated PKA signal [23], and transcription factor PPARγ [16].

Elevated xpression of ASS1, c-Myc, Axl, and Gas6 mRNA in primary cultures derived from ADI-PEG20-treated melanoma patients

We established two pairs of primary cultures from tumor biopsies of melanoma patients prior to ADI-PEG20 treatment and after failure of the treatment from the previous clinical study [13]. We determined mRNA levels of ASS1, c-Myc, Axl and Gas6 by quantitative real-time PCR in these cells. We found significantly increased expression of all these mRNA in cultured cells from ADI-resistant patients as compared correspondingly to those from patients prior to the treatment. In both patients, ASS1 and c-Myc mRNA levels were increased 2- to 8-fold, whereas Axl and Gas6 mRNA were increased 30 ~ 60% ($p < 0.05$, Fig. 7E). These results showed that within the limited available samples, elevated expression of ASS1, c-Myc, Axl, and Gas6 expression seems to associate with treatment failure of ADI in melanoma patients. Further studies using bigger samples are needed to validate this finding.

DISCUSSION

Arg auxotrophy provides a metabolic vulnerability for targeted therapy using Arg deprivation strategies in cancer chemotherapy. In this communication, we elucidated the molecular pathways underlying how cancer cells respond to Arg auxotrophic challenge and results are schematically depicted in Fig. 8. We demonstrated that ROS mobilization, which stimulates the Gas6/Axl signal, is a very early event in Arg-auxotrophic response. Gas6 is a vitamin K-dependent ligand for TAM receptor family which consists of Tyro3, Axl and Mer [52], and Axl has the highest affinity for Gas6 among all [38]. By interacting with its receptors, Gas6 plays important roles in multiple physiological and pathophysiological functions, including innate immunity, vasculature, atherosclosis, and thrombosis [35, 36]. Gas6 and Axl have been found overexpressed in many human malignancies (reviewed in references [35, 42, 60]), and that overexpression of Axl is correlated with poor prognosis for some cancers [15, 46]. Moreover, upregulation of Axl has been demonstrated to develop acquired resistance to many chemotherapeutics [42, 63], including inhibitors of epidermal growth factor receptor [4, 14, 66], BRAF[v600] (PLX4720) [26], and MEK (PD0325901 and AZD6244) [6]. The present results demonstrated that Axl is involved in regulation of ASS1 resulting in acquired resistance to Arg-deprivation chemotherapeutics, expanding the role of Axl in cancer chemotherapy.

Activation of Gas6/Axl in Arg-auxotrophic response is stimulated by ROS. This occurs within minutes. Additional support for the involvement ROS in Gas6/Axl signaling is provided by the use of antioxidant NAC which suppresses the activation and pro-oxidants which promotes the activation. It has recently been reported that prolong treatment (24 hr) of MDA-MB-231 cells with ADI induces ROS and mitochondrial fragmentation, leading to autophagy [44]. Our results suggested that generation of ROS is an early event that drives Arg-auxotrophic response of Gas6/Axl activation. However, how Arg starvation elicits ROS production requires further investigation.

Our results also demonstrated that activation of Axl signal by Arg starvation follows biphasic kinetics, *i.e.*, immediate-early activation by protein phosphorylation and subsequent transcriptional upregulation. Transcriptional upregulation of Axl is mediated by c-Myc which is also regulated by Arg-deprivation in a biphasic mode. Upregulated c-Myc then feeds back to enhance Axl transcription, thereby amplifying the downstream Ras signal. In the meantime, c-Myc also feeds forward to upregulate ASS1 expression (Fig. 8). Upregulated ASS1 not only promotes Arg biosynthesis to relieve Arg-auxotrophic pressure, but also feedbacks to downregulate c-Myc and Axl expression. This feedback mechanism provides a self-guarding mechanism for ASS1 homeostasis control because elevated expression of ASS1 may result in over-production of argininosuccinate, which is cytotoxic [10]. Furthermore, the self-regulatory mechanism of ASS1 may be an integral part of metabolic flux in urea cycle regulation. Recent study demonstrated that several enzymes in the urea cycle metabolism are co-regulated, including ASS1, argininosuccinate lyase, nitric oxide synthase, and cationic amino acid transporter 1 by forming a supermolecular complex that regulates metabolic flux [9]. Collectively, our present results and those described previously [37, 59] establish an intricate network consisting of inter-regulatory and self-regulatory loops that control Arg homeostasis (Fig. 8).

The multiple inter-regulatory loops place c-Myc in the center of the network, in which c-Myc plays a positive role in upregulating Axl and itself under Arg-depleting stress but a negative role of in regulating Axl and c-Myc when ASS1 expression is elevated. While the exact mechanisms underlying these differential regulation mechanisms are not clear at this time, however, this may not be surprising. C-Myc contains several highly conserved domains that are interactive with various binding partners (TRRAP, TIP60, TIP48, p400, Skp2, etc) that can function in positive and negative regulation modes [7, 20]. The carboxy-terminal region of c-Myc comprises the basic helix-loop-helix leucine zipper (bHLHz) domain which can dimerize with other bHLHz members that are essential for Myc's transcriptional regulation through E-box DNA binding. Dimerization of c-Myc and Max confers positive regulation [1, 33], whereas with MIZI (also known as ABTB1) mediates repression of target genes [62]. In addition, c-Myc can regulate rates of transcriptional elongation [45]. Further investigations are needed to elucidate how c-Myc performs bi-directional regulation in controlling the overall Arg-auxotrophic response. In a broader aspect, because c-Myc is involved in regulating 15 -20% of total genes in human genome [57, 61], Arg-auxotrophic response is likely to have effects on global cancer metabolism. Of note is that mechanisms of Gas6/Axl in Arg-auxotrophic involvement differ from those found in other amino acid depletions such as histidine, leucine [29, 51] or asparagine [28] which involve the conserved GCN2/elf2α and mTOR signaling [24, 30].

Our present findings may have the following important therapeutic implications. First, in addition to previously demonstrated ASS1 induction [58, 59], present study demonstrated that enhanced Gas6/Axl expression in cancer cell lines including those derived from melanoma patients suggest that Gas6/Axl are likely important prognostic markers for the treatment outcomes, although more studies are needed. Gas6 secretion is an early event of ADI treatment and Gas6 concentration in human plasma is lower than 0.5 nM [18, 53], therefore, development of highly sensitive Gas6 assay for liquid specimens will be very helpful. Second, Gas6/Axl may become viable targets in drug development for cancer chemotherapy.

We demonstrated that inhibitors to Gas6 (warfarin) and Axl (bosutinib) can suppress the Arg-auxotrophic effects and enhance the cell-killing ability of ADI in Arg-auxotrophic cells. Warfain (trade name: Coumadin, Jantoven, and Marevan) is a relatively safe FDA approved anti-thrombosis and anti-thromboembolism drug. Moreover, targeting Axl using small molecules [4, 22, 64] have been under clinical evaluations for cancer therapy. Third, these treatment developments are particularly compelling, because they can target malignant melanoma independently of BRAF mutations . Thus, our findings have important implications for improving the treatment efficacy of targeted therapy of Arg-auxotrophic tumors.

METHODS

Methods are in Supplementary, including: Reagents, Cell culture and Antibodies; Plasmid DNA Construction and shRNA Transfection; Phospho-RTK Array Analysis; Activated RAS pull-down Assay; Immunoprecipitation and Immunoblotting; Western blotting Analysis in Gas6 secretion; Detection of intracellular ROS; Establishment of primary cultures; Analysis of TCGA data; Other procedures including cytotoxicity determination using MTT or SRB (Life Technologies, Grand Island, NY) and DNA fragmentation (apoptosis) assays [58, 59].

Supplementary Material

Refer to Web version on PubMed Central for supplementary material.

ACKNOWLEDGEMENTS

REFERENCES

1. Amati B, Brooks MW, Levy N, Littlewood TD, Evan GI, Land H. Oncogenic activity of the c-Myc protein requires dimerization with Max. Cell. 1993; 72:233–245. [PubMed: 8425220]

2. Avilla E, Guarino V, Visciano C, Liotti F, Svelto M, Krishnamoorthy G, et al. Activation of TYRO3/AXL tyrosine kinase receptors in thyroid cancer. Cancer research. 2011; 71:1792–1804. [PubMed: 21343401]

3. Beaudet AL, O'Brien WE, Bock HG, Freytag SO, Su TS. The human argininosuccinate synthetase locus and citrullinemia. Advances in human genetics. 1986; 15:161–196. 291–162. [PubMed: 3513483]

4. Byers LA, Diao L, Wang J, Saintigny P, Girard L, Peyton M, et al. An epithelial-mesenchymal transition gene signature predicts resistance to EGFR and PI3K inhibitors and identifies Axl as a therapeutic target for overcoming EGFR inhibitor resistance. Clinical cancer research : an official journal of the American Association for Cancer Research. 2013; 19:279–290. [PubMed: 23091115]

5. Chardin P, McCormick F. Brefeldin A: the advantage of being uncompetitive. Cell. 1999; 97:153–155. [PubMed: 10219235]

6. Cirone P, Andresen CJ, Eswaraka JR, Lappin PB, Bagi CM. Patient-derived xenografts reveal limits to PI3K/mTOR- and MEK-mediated inhibition of bladder cancer. Cancer chemotherapy and pharmacology. 2014; 73:525–538. [PubMed: 24442130]

7. Conacci-Sorrell M, McFerrin L, Eisenman RN. An overview of MYC and its interactome. Cold Spring Harbor perspectives in medicine. 2014; 4:a014357. [PubMed: 24384812]

8. Ekman C, Stenhoff J, Dahlback B. Gas6 is complexed to the soluble tyrosine kinase receptor Axl in human blood. J Thromb Haemost. 2010; 8:838–844. [PubMed: 20088931]

9. Erez A, Nagamani SC, Shchelochkov OA, Premkumar MH, Campeau PM, Chen Y, et al. Requirement of argininosuccinate lyase for systemic nitric oxide production. Nature medicine. 2011; 17:1619–1626.

10. Erez A. Argininosuccinic aciduria: from a monogenic to a complex disorder. Genetics in medicine : official journal of the American College of Medical Genetics. 2013; 15:251–257. [PubMed: 23306800]

11. Feneyrolles C, Spenlinhauer A, Guiet L, Fauvel B, Dayde-Cazals B, Warnault P, et al. Axl kinase as a key target for oncology: focus on small molecule inhibitors. Molecular cancer therapeutics. 2014; 13:2141–2148. [PubMed: 25139999]

12. Feun L, Savaraj N. Pegylated arginine deiminase: a novel anticancer enzyme agent. Expert opinion on investigational drugs. 2006; 15:815–822. [PubMed: 16787144]

13. Feun LG, Marini A, Walker G, Elgart G, Moffat F, Rodgers SE, et al. Negative argininosuccinate synthetase expression in melanoma tumours may predict clinical benefit from arginine-depleting therapy with pegylated arginine deiminase. British journal of cancer. 2012; 106:1481–1485. [PubMed: 22472884]

14. Giles KM, Kalinowski FC, Candy PA, Epis MR, Zhang PM, Redfern AD, et al. Axl mediates acquired resistance of head and neck cancer cells to the epidermal growth factor receptor inhibitor erlotinib. Molecular cancer therapeutics. 2013; 12:2541–2558. [PubMed: 24026012]

15. Gjerdrum C, Tiron C, Hoiby T, Stefansson I, Haugen H, Sandal T, et al. Axl is an essential epithelial-to-mesenchymal transition-induced regulator of breast cancer metastasis and patient survival. Proceedings of the National Academy of Sciences of the United States of America. 2010; 107:1124–1129. [PubMed: 20080645]

16. Goodwin BL, Corbin KD, Pendleton LC, Levy MM, Solomonson LP, Eichler DC. Troglitazone up-regulates vascular endothelial argininosuccinate synthase. Biochemical and biophysical research communications. 2008; 370:254–258. [PubMed: 18375203]

17. Graham DK, DeRyckere D, Davies KD, Earp HS. The TAM family: phosphatidylserine-sensing receptor tyrosine kinases gone awry in cancer. Nature reviews Cancer. 2014; 14:769–785. [PubMed: 25568918]

18. Griffin JH, Gruber A, Fernandez JA. Reevaluation of total, free, and bound protein S and C4b-binding protein levels in plasma anticoagulated with citrate or hirudin. Blood. 1992; 79:3203–3211. [PubMed: 1534488]

19. Haines RJ, Corbin KD, Pendleton LC, Eichler DC. Protein kinase Calpha phosphorylates a novel argininosuccinate synthase site at serine 328 during calcium-dependent stimulation of endothelial nitric-oxide synthase in vascular endothelial cells. The Journal of biological chemistry. 2012; 287:26168–26176. [PubMed: 22696221]

20. Hara K, Yonezawa K, Weng QP, Kozlowski MT, Belham C, Avruch J. Amino acid sufficiency and mTOR regulate p70 S6 kinase and eIF-4E BP1 through a common effector mechanism. The Journal of biological chemistry. 1998; 273:14484–14494. [PubMed: 9603962]

21. Holbrook AM, Pereira JA, Labiris R, McDonald H, Douketis JD, Crowther M, et al. Systematic overview of warfarin and its drug and food interactions. Arch Intern Med. 2005; 165:1095–1106. [PubMed: 15911722]

22. Holland SJ, Pan A, Franci C, Hu Y, Chang B, Li W, et al. R428, a selective small molecule inhibitor of Axl kinase, blocks tumor spread and prolongs survival in models of metastatic breast cancer. Cancer research. 2010; 70:1544–1554. [PubMed: 20145120]

23. Huang Z, Wang TS, Zhao YC, Zuo RJ, Deng WB, Chi YJ, et al. Cyclic adenosine monophosphate-induced argininosuccinate synthase 1 expression is essential during mouse decidualization. Molecular and cellular endocrinology. 2014; 388:20–31. [PubMed: 24556046]

24. Jackson RJ, Hellen CU, Pestova TV. The mechanism of eukaryotic translation initiation and principles of its regulation. Nature reviews Molecular cell biology. 2010; 11:113–127. [PubMed: 20094052]

25. Jakob S, Schroeder P, Lukosz M, Buchner N, Spyridopoulos I, Altschmied J, et al. Nuclear protein tyrosine phosphatase Shp-2 is one important negative regulator of nuclear export of telomerase

reverse transcriptase. The Journal of biological chemistry. 2008; 283:33155–33161. [PubMed: 18829466]

26. Johannessen CM, Boehm JS, Kim SY, Thomas SR, Wardwell L, Johnson LA, et al. COT drives resistance to RAF inhibition through MAP kinase pathway reactivation. Nature. 2010; 468:968–972. [PubMed: 21107320]

27. Khoury HJ, Cortes JE, Kantarjian HM, Gambacorti-Passerini C, Baccarani M, Kim DW, et al. Bosutinib is active in chronic phase chronic myeloid leukemia after imatinib and dasatinib and/or nilotinib therapy failure. Blood. 2012; 119:3403–3412. [PubMed: 22371878]

28. Kilberg MS, Balasubramanian M, Fu L, Shan J. The transcription factor network associated with the amino acid response in mammalian cells. Advances in nutrition. 2012; 3:295–306. [PubMed: 22585903]

29. Kimball SR, Horetsky RL, Jefferson LS. Implication of eIF2B rather than eIF4E in the regulation of global protein synthesis by amino acids in L6 myoblasts. The Journal of biological chemistry. 1998; 273:30945–30953. [PubMed: 9812990]

30. Kimball SR, Jefferson LS. Control of translation initiation through integration of signals generated by hormones, nutrients, and exercise. J Biol Chem. 2010; 285:29027–29032. [PubMed: 20576612]

31. Kodigepalli KM, Bowers K, Sharp A, Nanjundan M. Roles and regulation of phospholipid scramblases. FEBS letters. 2015; 589:3–14. [PubMed: 25479087]

32. Konishi A, Aizawa T, Mohan A, Korshunov VA, Berk BC. Hydrogen peroxide activates the Gas6-Axl pathway in vascular smooth muscle cells. The Journal of biological chemistry. 2004; 279:28766–28770. [PubMed: 15123721]

33. Kretzner L, Blackwood EM, Eisenman RN. Myc and Max proteins possess distinct transcriptional activities. Nature. 1992; 359:426–429. [PubMed: 1406956]

34. Kuo MT, Savaraj N, Feun LG. Targeted cellular metabolism for cancer chemotherapy with recombinant arginine-degrading enzymes. Oncotarget. 2010; 1:246–251. [PubMed: 21152246]

35. Laurance S, Lemarie CA, Blostein MD. Growth arrest-specific gene 6 (gas6) and vascular hemostasis. Advances in nutrition. 2012; 3:196–203. [PubMed: 22516727]

36. Lemke G. Biology of the TAM receptors. Cold Spring Harbor perspectives in biology. 2013; 5:a009076. [PubMed: 24186067]

37. Long Y, Tsai WB, Wangpaichitr M, Tsukamoto T, Savarah N, Feun LG, et al. Arginine Deiminase Resistance in Melanoma Cells Is Associated with Metabolic Reprogramming, Glucose Dependence and Glutamine Addiction. Molecular cancer therapeutics. 2013

38. Nagata K, Ohashi K, Nakano T, Arita H, Zong C, Hanafusa H, et al. Identification of the product of growth arrest-specific gene 6 as a common ligand for Axl, Sky, and Mer receptor tyrosine kinases. The Journal of biological chemistry. 1996; 271:30022–30027. [PubMed: 8939948]

39. Neel BG, Gu H, Pao L. The 'Shp'ing news: SH2 domain-containing tyrosine phosphatases in cell signaling. Trends in biochemical sciences. 2003; 28:284–293. [PubMed: 12826400]

40. Nickel W. Pathways of unconventional protein secretion. Current opinion in biotechnology. 2010; 21:621–626. [PubMed: 20637599]

41. Ou WB, Hubert C, Corson JM, Bueno R, Flynn DL, Sugarbaker DJ, et al. Targeted inhibition of multiple receptor tyrosine kinases in mesothelioma. Neoplasia. 2011; 13:12–22. [PubMed: 21245936]

42. Paccez JD, Vogelsang M, Parker MI, Zerbini LF. The receptor tyrosine kinase Axl in cancer: biological functions and therapeutic implications. International journal of cancer Journal international du cancer. 2014; 134:1024–1033. [PubMed: 23649974]

43. Phillips MM, Sheaff MT, Szlosarek PW. Targeting arginine-dependent cancers with arginine-degrading enzymes: opportunities and challenges. Cancer research and treatment : official journal of Korean Cancer Association. 2013; 45:251–262. [PubMed: 24453997]

44. Qiu F, Chen YR, Liu X, Chu CY, Shen LJ, Xu J, et al. Arginine Starvation Impairs Mitochondrial Respiratory Function in ASS1-Deficient Breast Cancer Cells. Science signaling. 2014; 7:ra31. [PubMed: 24692592]

45. Rahl PB, Lin CY, Seila AC, Flynn RA, McCuine S, Burge CB, et al. c-Myc regulates transcriptional pause release. Cell. 2010; 141:432–445. [PubMed: 20434984]

46. Rochlitz C, Lohri A, Bacchi M, Schmidt M, Nagel S, Fopp M, et al. Axl expression is associated with adverse prognosis and with expression of Bcl-2 and CD34 in de novo acute myeloid leukemia (AML): results from a multicenter trial of the Swiss Group for Clinical Cancer Research (SAKK). Leukemia. 1999; 13:1352–1358. [PubMed: 10482985]

47. Saenz JB, Sun WJ, Chang JW, Li J, Bursulaya B, Gray NS, et al. Golgicide A reveals essential roles for GBF1 in Golgi assembly and function. Nat Chem Biol. 2009; 5:157–165. [PubMed: 19182783]

48. Sasaki T, Knyazev PG, Cheburkin Y, Gohring W, Tisi D, Ullrich A, et al. Crystal structure of a C-terminal fragment of growth arrest-specific protein Gas6. Receptor tyrosine kinase activation by laminin G-like domains. The Journal of biological chemistry. 2002; 277:44164–44170. [PubMed: 12218057]

49. Sasaki T, Knyazev PG, Clout NJ, Cheburkin Y, Gohring W, Ullrich A, et al. Structural basis for Gas6-Axl signalling. The EMBO journal. 2006; 25:80–87. [PubMed: 16362042]

50. Segawa K, Suzuki J, Nagata S. Flippases and scramblases in the plasma membrane. Cell cycle. 2014; 13:2990–2991. [PubMed: 25486557]

51. Shan J, Fu L, Balasubramanian MN, Anthony T, Kilberg MS. ATF4-dependent regulation of the JMJD3 gene during amino acid deprivation can be rescued in Atf4-deficient cells by inhibition of deacetylation. The Journal of biological chemistry. 2012; 287:36393–36403. [PubMed: 22955275]

52. Stitt TN, Conn G, Gore M, Lai C, Bruno J, Radziejewski C, et al. The anticoagulation factor protein S and its relative, Gas6, are ligands for the Tyro 3/Axl family of receptor tyrosine kinases. Cell. 1995; 80:661–670. [PubMed: 7867073]

53. Suh CH, Hilliard B, Li S, Merrill JT, Cohen PL. TAM receptor ligands in lupus: protein S but not Gas6 levels reflect disease activity in systemic lupus erythematosus. Arthritis research & therapy. 2010; 12:R146. [PubMed: 20637106]

54. Suzuki J, Nagata S. Phospholipid scrambling on the plasma membrane. Methods in enzymology. 2014; 544:381–393. [PubMed: 24974298]

55. Syed N, Langer J, Janczar K, Singh P, Lo Nigro C, Lattanzio L, et al. Epigenetic status of argininosuccinate synthetase and argininosuccinate lyase modulates autophagy and cell death in glioblastoma. Cell death & disease. 2013; 4:e458. [PubMed: 23328665]

56. Trask PC, Cella D, Besson N, Kelly V, Masszi T, Kim DW. Health-related quality of life of bosutinib (SKI-606) in imatinib-resistant or imatinib-intolerant chronic phase chronic myeloid leukemia. Leukemia research. 2012; 36:438–442. [PubMed: 22036634]

57. Trask PC, Cella D, Powell C, Reisman A, Whiteley J, Kelly V. Health-related quality of life in chronic myeloid leukemia. Leukemia research. 2013; 37:9–13. [PubMed: 23116602]

58. Tsai WB, Aiba I, Lee SY, Feun L, Savaraj N, Kuo MT. Resistance to arginine deiminase treatment in melanoma cells is associated with induced argininosuccinate synthetase expression involving c-Myc/HIF-1alpha/Sp4. Molecular cancer therapeutics. 2009; 8:3223–3233. [PubMed: 19934275]

59. Tsai WB, Aiba I, Long Y, Lin HK, Feun L, Savaraj N, et al. Activation of Ras/PI3K/ERK pathway induces c-Myc stabilization to upregulate argininosuccinate synthetase, leading to arginine deiminase resistance in melanoma cells. Cancer research. 2012; 72:2622–2633. [PubMed: 22461507]

60. Verma A, Warner SL, Vankayalapati H, Bearss DJ, Sharma S. Targeting Axl and Mer kinases in cancer. Molecular cancer therapeutics. 2011; 10:1763–1773. [PubMed: 21933973]

61. Walz S, Lorenzin F, Morton J, Wiese KE, von Eyss B, Herold S, et al. Activation and repression by oncogenic MYC shape tumour-specific gene expression profiles. Nature. 2014; 511:483–487. [PubMed: 25043018]

62. Wiese KE, Walz S, von Eyss B, Wolf E, Athineos D, Sansom O, et al. The role of MIZ-1 in MYC-dependent tumorigenesis. Cold Spring Harbor perspectives in medicine. 2013; 3:a014290. [PubMed: 24296348]

63. Wu X, Liu X, Koul S, Lee CY, Zhang Z, Halmos B. AXL kinase as a novel target for cancer therapy. Oncotarget. 2014; 5:9546–9563. [PubMed: 25337673]

64. Ye X, Li Y, Stawicki S, Couto S, Eastham-Anderson J, Kallop D, et al. An anti-Axl monoclonal antibody attenuates xenograft tumor growth and enhances the effect of multiple anticancer therapies. Oncogene. 2010; 29:5254–5264. [PubMed: 20603615]

65. Zhang YX, Knyazev PG, Cheburkin YV, Sharma K, Knyazev YP, Orfi L, et al. AXL is a potential target for therapeutic intervention in breast cancer progression. Cancer research. 2008; 68:1905–1915. [PubMed: 18339872]

66. Zhang Z, Lee JC, Lin L, Olivas V, Au V, LaFramboise T, et al. Activation of the AXL kinase causes resistance to EGFR-targeted therapy in lung cancer. Nature genetics. 2012; 44:852–860. [PubMed: 22751098]
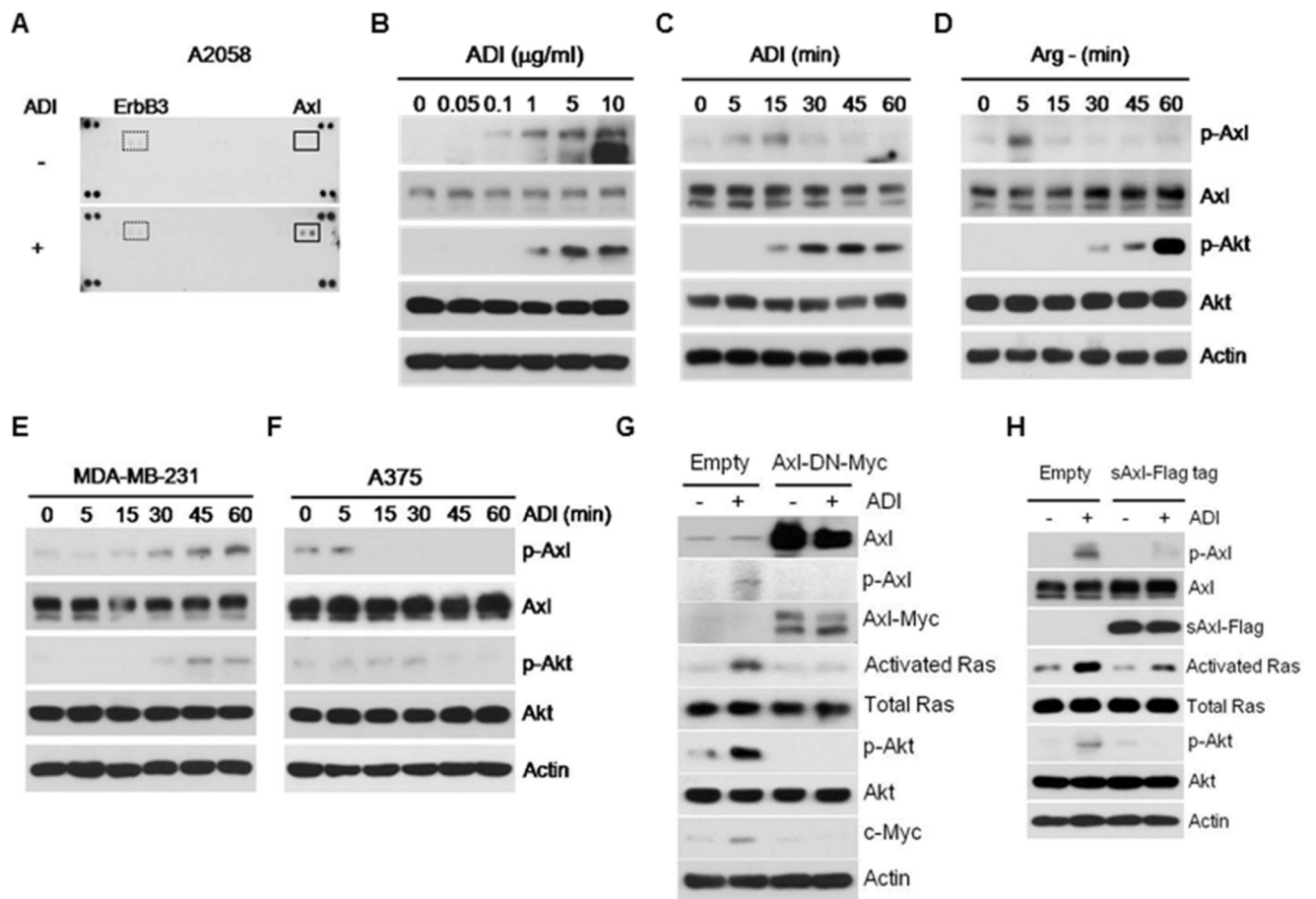
Figure 1.
Activation of Axl in response to ADI-PEG20. **A,** activation of Axl by ADI assayed by a phospho-RTK array. **B,** Western blots showing dose-dependent activation of Axl by ADI in A2058 cells. **C** and **D,** time-dependent activation of Axl in A2058 cells treated with ADI **(C)** or grown in Arg-free medium **(D)**. **E** and **F,** time-dependent regulation of Axl in MDA-MB-231 and A375 cells by ADI, respectively. **G** and **H,** suppression of Axl activation by dominant-negative Axl mutant and by sAxl, respectively.
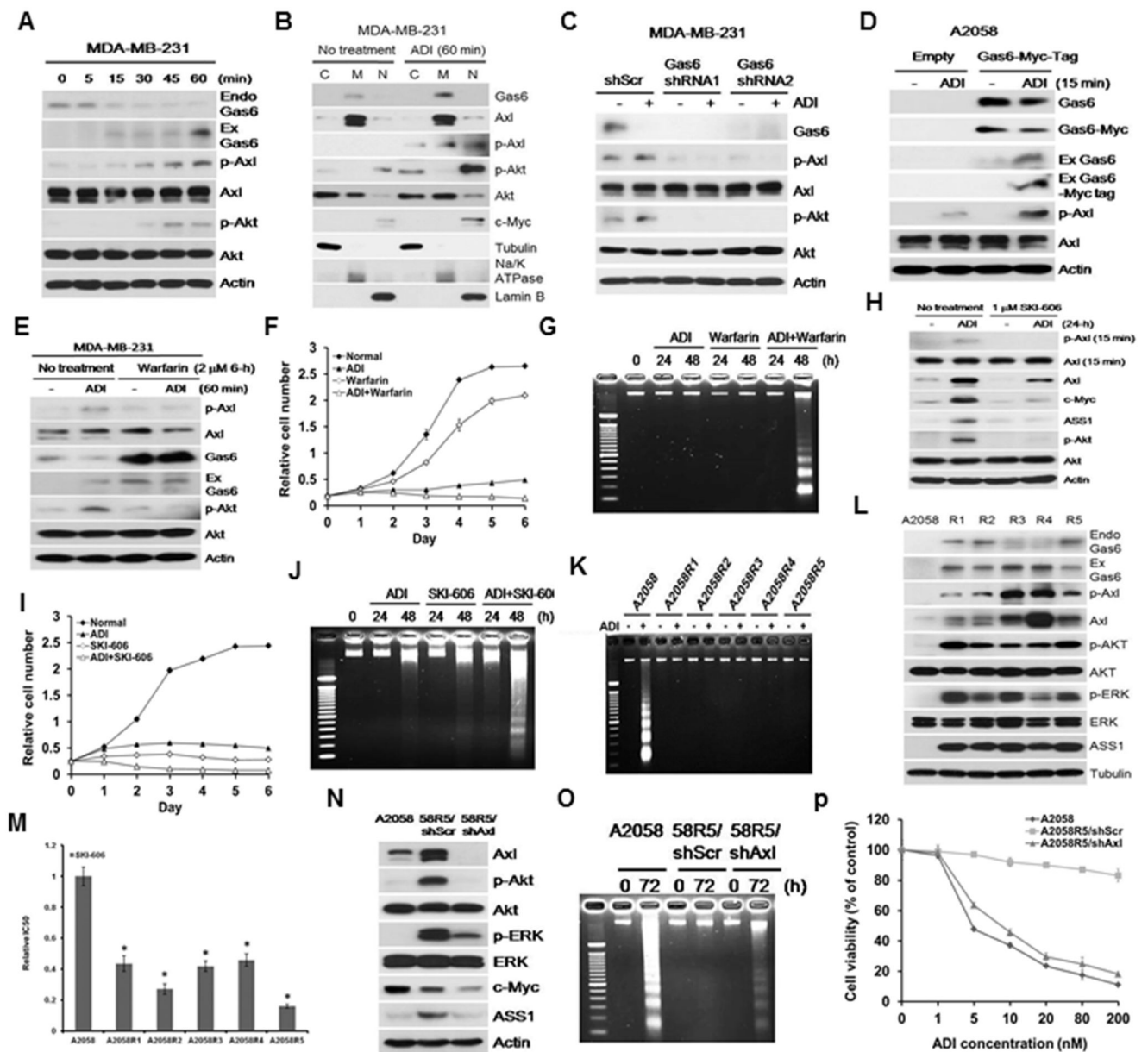
Figure 2.
Roles of Gas6 in Axl activation by ADI. **A**, time-dependent secretion of Gas6 by ADI;
Endo, endogenous; Ex, ectopic. MDA-MB-231 cells were used because of detectable Gas6
level as compared with A2058 cells. **B**, distributions of Gas6 by subcellular fractionation
into cytoplasmic (C), cytoplasmic membrane (M) and nuclear fractions (N), using their
respective markers as indicated in the text. **C**, suppression of ADI-induced Axl activation by
Gas6 shRNA. **D**, activation of Axl by transfected Myc-tagged Gas6. **E**, inhibition of Axl
activation by warfarin. **F** and **G**, additive effects of warfarin and ADI in cell-killing on
A2058 cells as determined by the SRB and DNA fragmentation assays, respectively. **H**,
suppression of Axl activation and c-Myc expression in A2058 cells treated with SKI-606 for
24-h. **I** and **J**, additive effects of SKI-606 (2 μM) and ADI for 72 hr as assayed by SRB and

by DNA fragmentation, respectively. **K**, DNA fragmentation assay in A2058 and its 5 ADI[R] cell lines treated with ADI. **L**, elevated expression of Gas6, Axl and their downstream signals in the 5 ADI[R] cell lines. **M**, Sensitivity of A2058 and its ADI[R] cells to SKI-606. Cells were incubated with SKI-606 at concentrations ranging from 0.1 to 10 μM for 48 h and their viabilities were determined by MTT assay. **N**, Knockdown of Axl by shAxl suppresses downstream signals in the representative ADI[R] cell lines (A2058R5). **O** and **P**, enhanced cell killing by ADI as assayed by DNA fragmentation (O) and cytotoxicity assay by MTT (P), respectively.
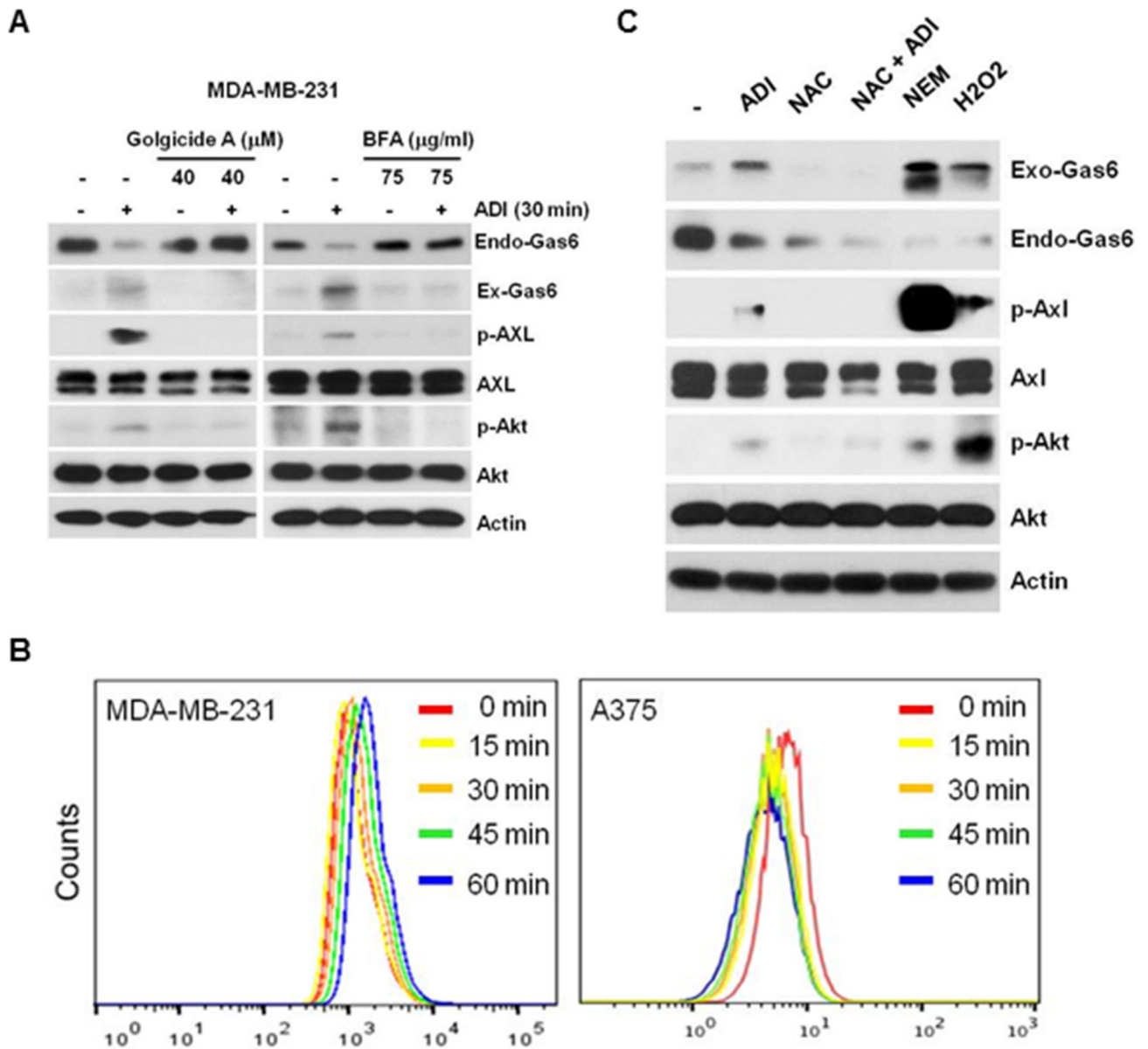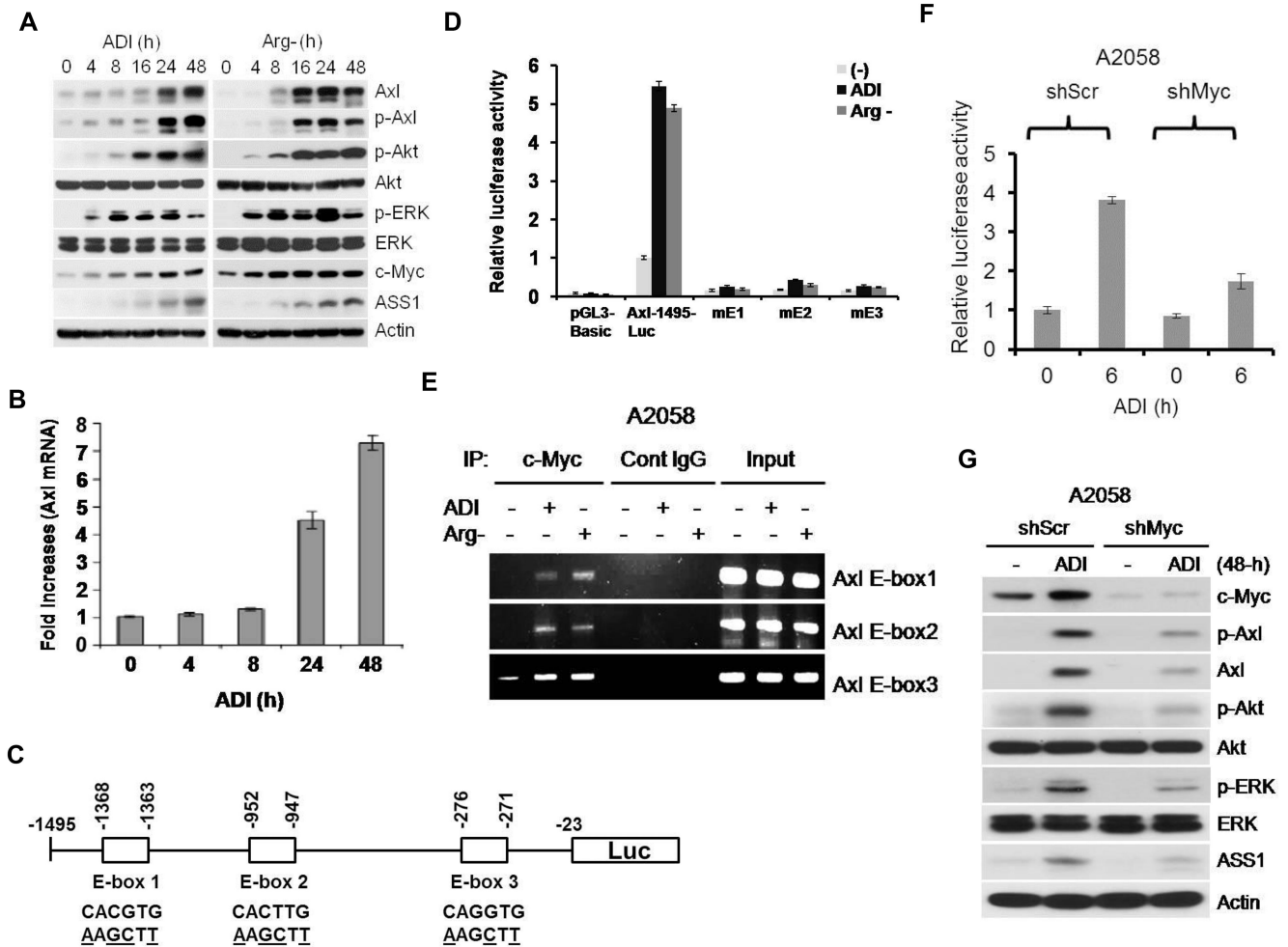
Figure 3.
Mechanism of Gas6/Axl activation by ADI. **A**, inhibition of Axl and its downstream effectors by Golgicide A (40 μM for 30 min, left) and BFA (75 μM for 30 min, right). MDA-MB-231 cells were used here because of detectable Gas6 level as compared with A2058 cells. **B**, measurements of ROS by DHR in MDA-MB-231 (left) and A375 cells (right) treated with ADI (0.5 μg/ml) for the time intervals as indicated. Results are representative of three independent experiments. **C**, effects of anti-oxidant on ADI-induced Gas6/Axl signal. MDA-MB-231 cells were pretreated with 100 μM NAC for 4 hr in the absence or presence of ADI for 1-h. MDA-MB-231 cells were also treated with NEM or H_2O_2, 100 μM each for 1 h. Expression levels of p-Axl, Axl, Gas6, pT[308]-AKT, Akt, and actin were analyzed by Western blotting.
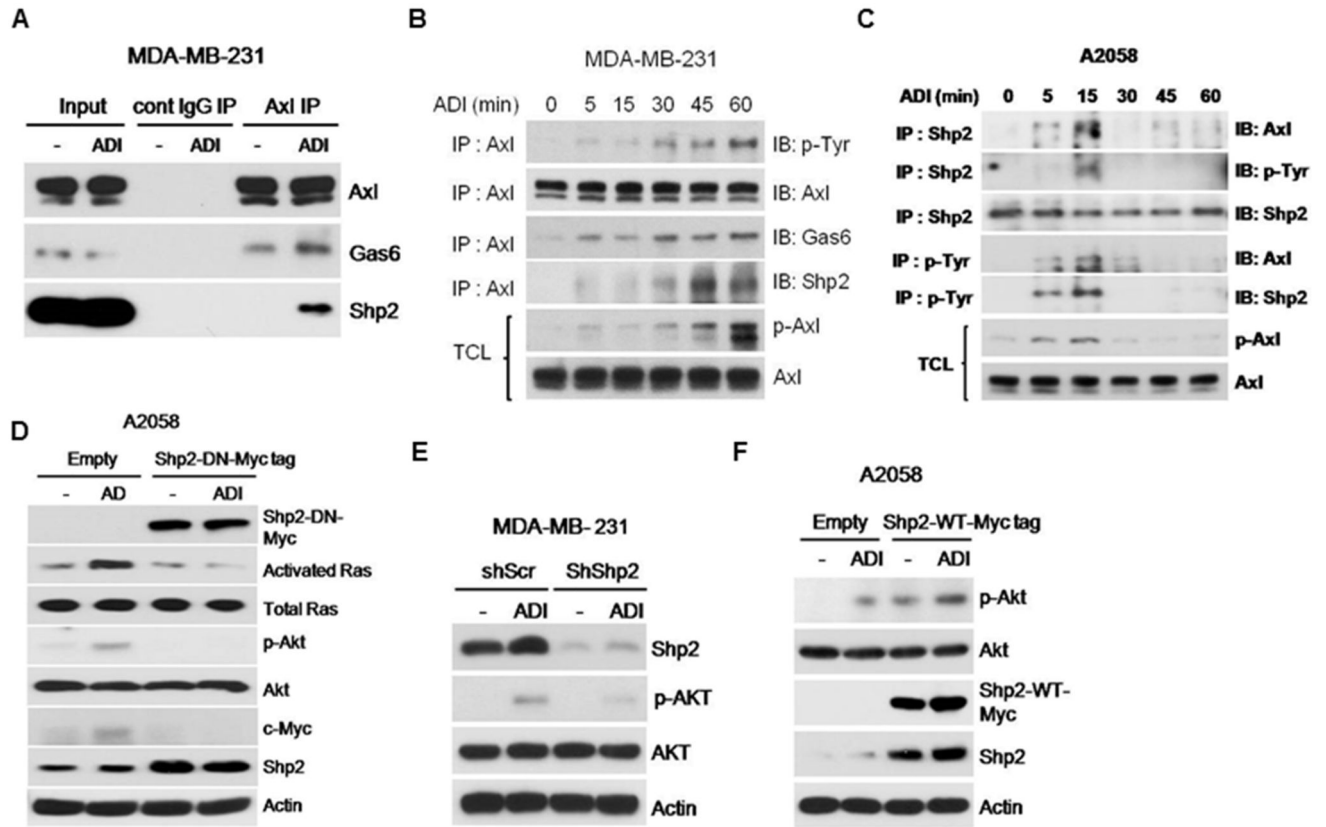
Figure 4.
Importance of Shp2 to the activated Gas6/Axl signal. **A**, ADI treatment enhances association of Axl, Gas6 and Shp2. Lysates from cells treated with or without ADI were immunoprecipitated with anti-Axl antibody followed by immunoblotting using antibodies as indicated. **B**, time-course induction of Shp2 association with Gas6/Axl treated with ADI. Cell lysates were immunoprecipitated with anti-Axl antibody followed by immunoblotting using antibodies as indicated. **C**, co-IP of Shp2 and Axl using anti-Shp2 or anti-phosphotyrosine antibodie (p-Tyr) in IP followed by immunoblotting with antibodies as indicated. TCL, total cell lysates. **D**, suppression of ADI-induced Ras/Akt activation and c-Myc upregulation by the dominant-negative Shp2. E, suppression of ADI-induced Akt activation by Shp2 shRNA. **F**, enhancement of ADI-induced Akt activation in Shp2-overexpressing cells. MDA-MB-231 cells were used in A, B, because of detectable Gas6 level as compared with A2058 cells.

Figure 5.

c-Myc is involved in transcriptional regulation of Axl expression by Arg-deprivation stress. **A**, enhanced Axl and c-Myc expression in A2058 cells treated ADI (left) or grown in Arg-free medium. **B**, quantitative real-time PCR analyses of Axl expression in A2058 cells treated with ADI. The results were from three independent experiments. **C**, schematic diagram of Axl-1495-luc reporter. Locations of 3 E-boxes with wild-type and mutated sequences are indicated. **D**, E-box-dependent activation of *Axl* promoter activity by Arg deprivation. A2058 cells were transfected with pGL3-Basic, wild-type Axl-1495-Luc, and mutant version and maintained in normal medium, medium containing ADI or Arg-free medium for 6 h. The *Axl* promoter activity was analyzed. **E**, ChIP assay of c-Myc binding to the 3 E-boxes in the *Axl* promoter. Cont, control. **F**, effects of c-Myc shRNA on the Axl promoter activity by ADI. The cells were transfected with c-Myc shRNA and its control scramble shRNA for 48 h. Cells were treated with ADI for 6-h. The *Axl* promoter activity was analyzed and normalized with that of the wild-type Axl-1495-Luc vector. **G**, effects of c-Myc shRNA on the activation of Axl/Akt/ERK by ADI. A2058 cells were transfected with c-Myc shRNA and its scramble control (shScr) for 48 h. Cells were treated with ADI for 48 h. Cell lysates were analyzed for the indicated proteins by Western blotting. The error bars

represent standard deviations from three independent experiments. A2058 cells were used because here because of low basal levels of Axl expression.
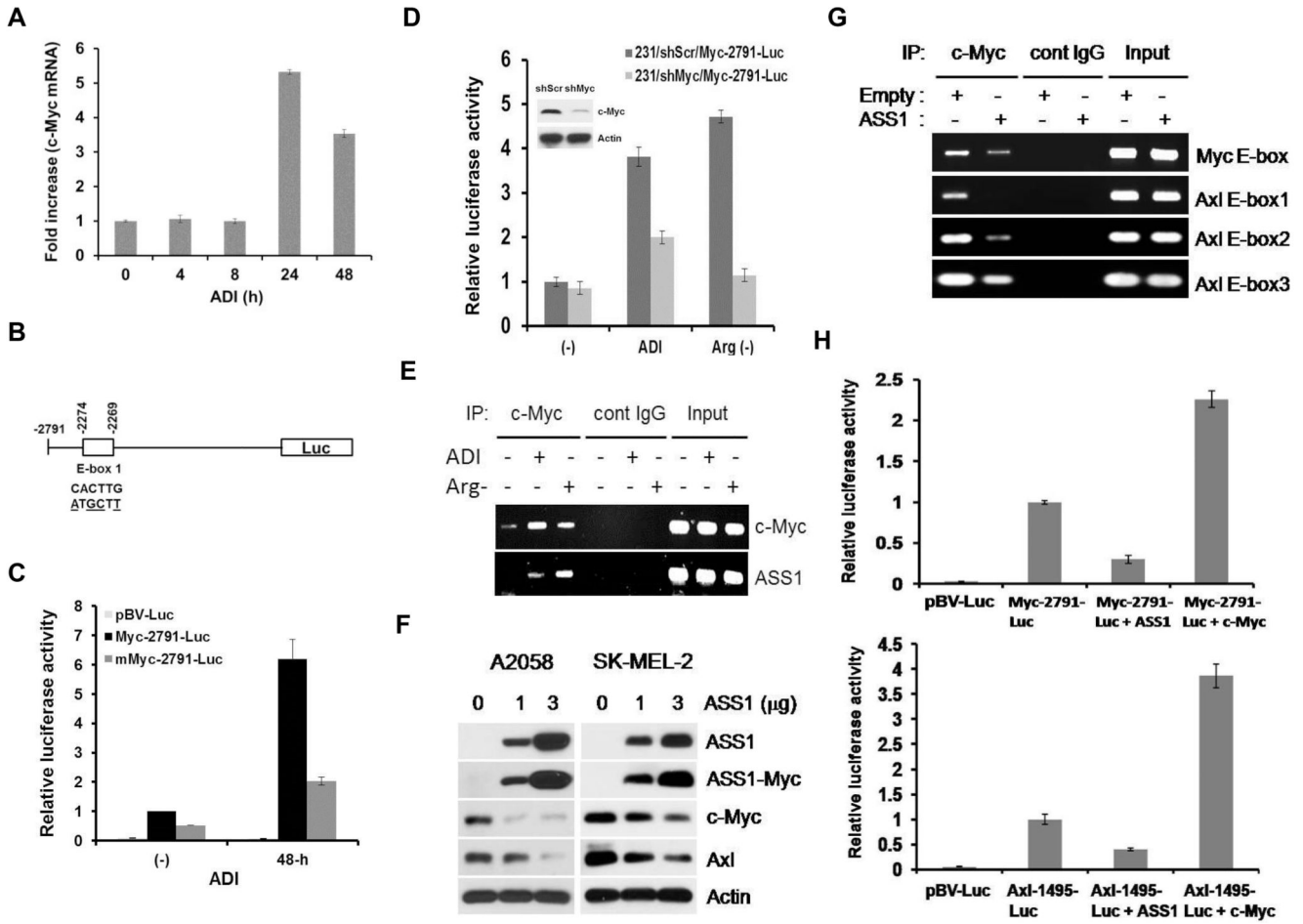
Figure 6.
Inter-regulatory network in Arg-auxotrophic response. **A**, quantitative real-time PCR measurement of c-Myc mRNA in A2058 cells treated with ADI for the time intervals as indicated. Results are from three independent experiments. **B**, schematic of the c-Myc-2791-luc construct in which wild-type and mutant E-boxes sequences are indicated. **C**, E-box-dependent activation of *c-Myc* promoter by ADI in A2058 cells. **D**, effects of c-Myc shRNA on the c-Myc promoter activity by ADI in the reporter assay in MDA-MB-231 cells. Cells were transfected with c-Myc shRNA or scramble shRNA (shScr) for 24 hr and treated with ADI or grown in Arg-free medium for 24 hr. Luc activities were determined from cell lysates. **E**, ChIP assay of c-Myc binding to the *c-Myc* promoter in 2058 cells treated with Arg-deprivation conditions. Input, genomic DNA prior to IP. **F**, inhibition of c-Myc and Axl expression by overexpressed ASS1 in A2058 and SK-MEL-2 cells. Cells were transfected with 1 and 3 μg of ASS1-Myc-Tag recombinant for 24-hr. Expression levels of ASS1, ASS1-Myc-tag, c-Myc, Axl, and Actin were analyzed by Western blotting. **G**, suppression of c-Myc binding to the E-box and 3 E-boxes located at the c-*Myc* and the *Axl* promoter in A2058 cells as determined by ChIP assay. **H,** inhibition of *c-Myc* (upper) and *Axl* (lower) promoter activity by overexpressed ASS1 in transfection assay. The *ASS1*-expressing recombinant was co-transfected with Myc-2791-Luc, Axl-1494-luc, or empty vector pGV-

luc into MDA-MB-231 cells. Expression of the reporters was measured and normalized to those without overexpression ASS1 as 1. Error bars represent standard deviations from three independent experiments. Melanoma cells A2058 or SK-MEL-2 cells were used here because of their low basal ASS1 expression.
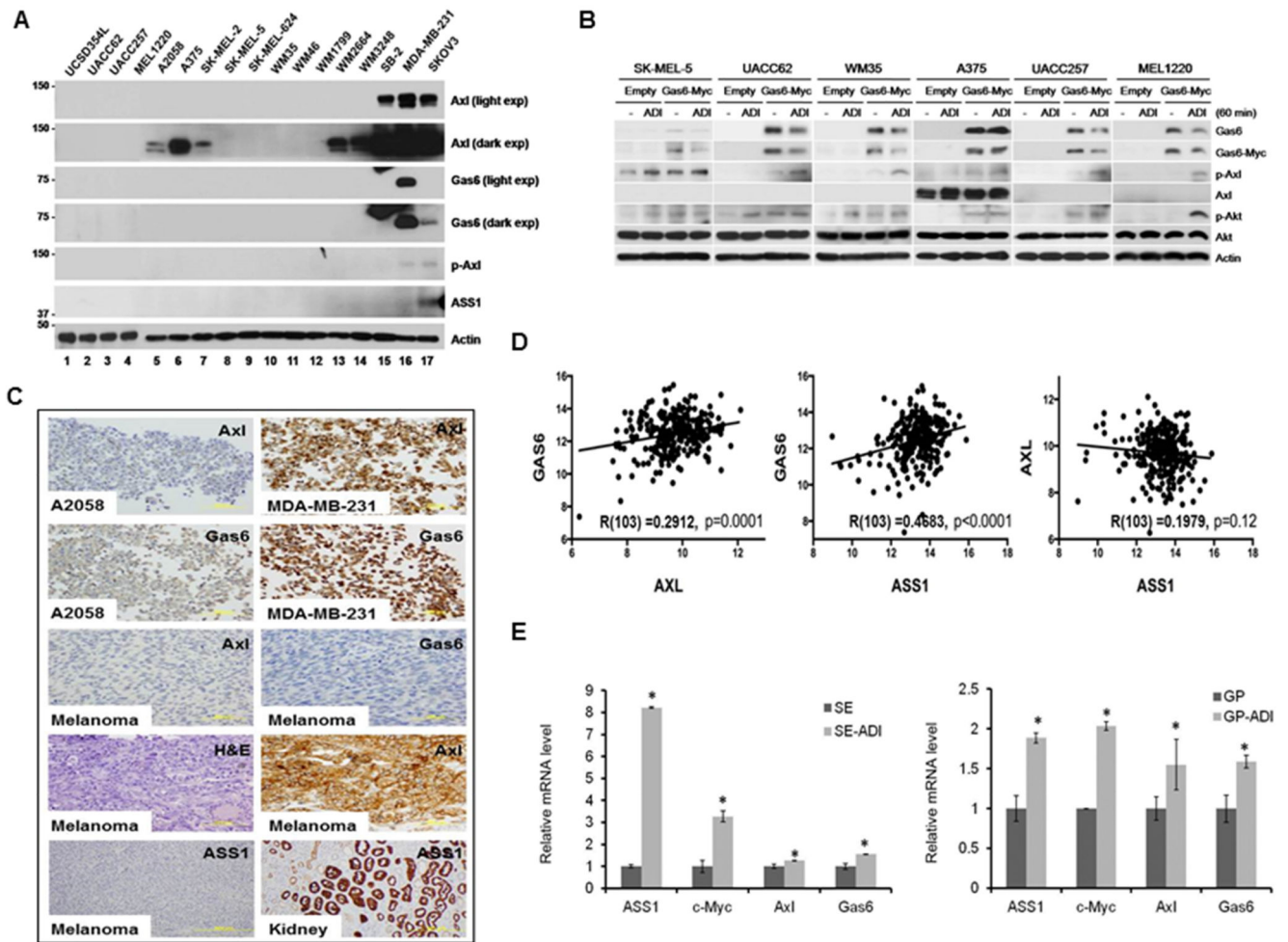
Figure 7.
Gas6 and Axl expression in melanoma cell lines and tissue specimens. **A**, immunoblots of melanoma (lanes 1-15), MDA-MB-231 (lane 16) and SKOV3 (lane 17) cell lines. **B**, activation of Axl by overexpressed Gas6 in six melanoma cancer cell lines. **C**, immunohistochemical staining of the melanoma cell lines A2058 (negative control for Axl and Gas6) and MDA-MB-231 (positive control) and Kidney tissue (positive control for Axl) and representative melanoma tissue sections with Gas6, Axl and ASS1 antibodies as indicated. H&E image is used to rule out the possibility of melanin involvement in IHC staining. **D**. positive correlation between Gas6 and Axl (left) and between Gas6 and ASS1 mRNA (middle), and between ASS1 and Axl mRNA levels (right) from 103 cases of cutaneous melanoma metastases in TCGA dataset. R, correlation coefficient. **E**. elevated expression of ASS1, c-Myc, Axl, and Gas6 mRNA in the primary cell cultures derived from two melanoma patients (SE and GP) before and after failed by ADI treatments as determined by quantitative real-time PCR. Data were presented as mean ± SD of three independent experiments. $*p < 0.05$ by the student's t-test.
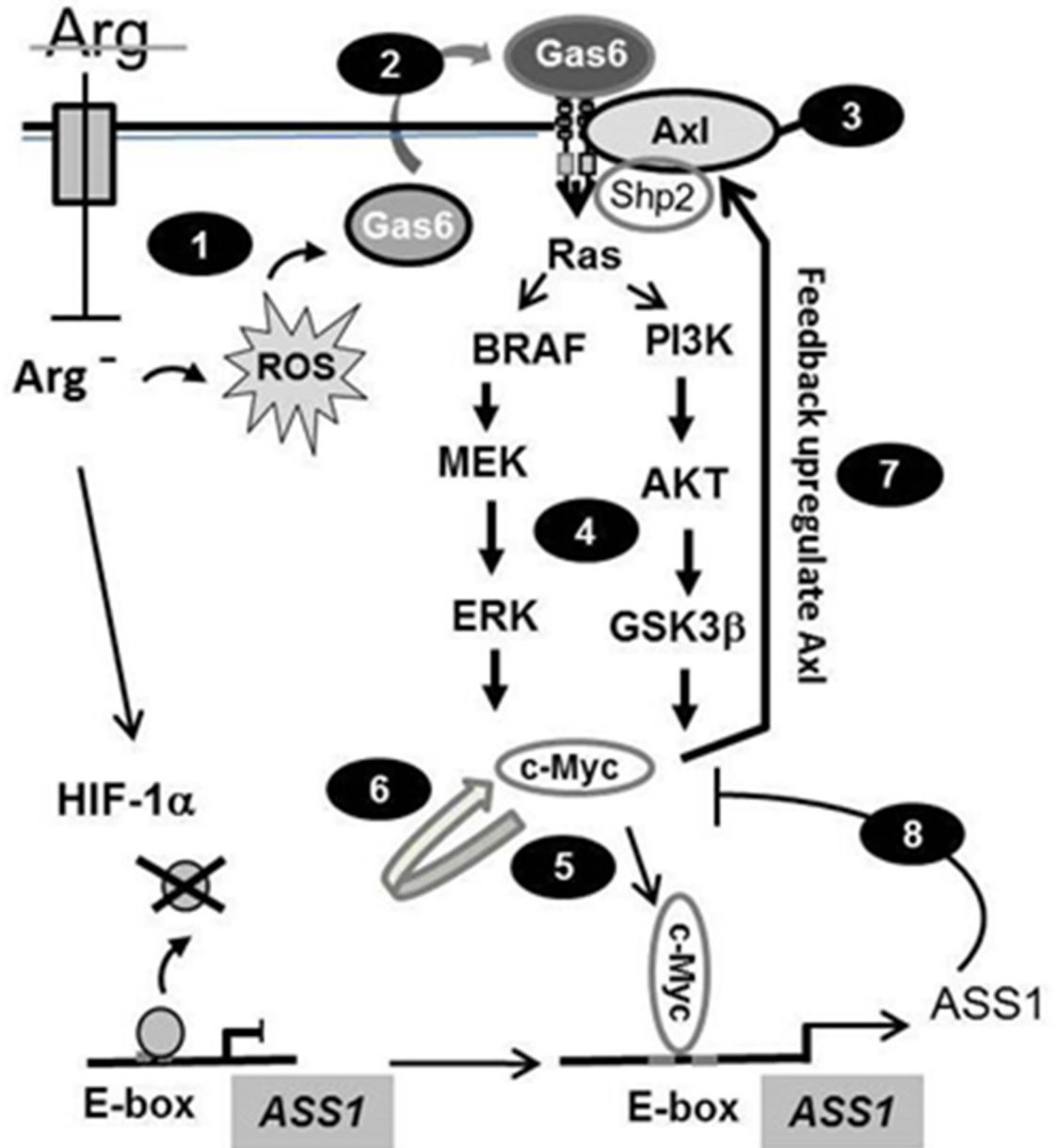
Figure 8.
Schematic depicting the Arg-auxotrophic response. 1) induction of ROS production, 2) Gas6 secretion and activation of Axl, 3) association of Shp2 with Gas6/Axl , 4) activation of the Ras/PI3K/Akt/ERK/c-Myc pathway, 5) c-Myc binding to the E-box of *ASS1* promoter and transcriptionally upregulating *ASS1*, 6) self-regulation of c-Myc, 7) feedback regulation of Axl by c-Myc, and 8) feedback inhibition of *c-Myc* and *Axl* expression by elevated ASS1. De-repression of HIF-1α from the E-box of *ASS1* promoter by ADI is also indicated.